Optical and Electrical Properties of Graphene Percolated Networks from Liquid Exfoliation of Graphite

J. Obrzut[a], D. Pristinski[a] and M. Yoonessi[b]

[a] Polymers Division, National Institute of Standards and Technology, Gaithersburg, MD 20899, USA
[b] Ohio Aerospace Instititute, Cleveland, OH 44135, USA

Thin films obtained from liquid phase exfoliation of graphite exhibit the conductivity and transparency properties of percolated networks having an interconnectivity distance of about 2 μm to 3 μm. The mean radius of the platelets in solution determined by dynamic light scattering measurements was found to be in the range of about 3 μm. Representative transmittance electron microscope images show evidence of individual graphene sheets. The platelets have an irregular shape with apparent folding and bending, which contributes to disorder and imperfections of the films as revealed by the Raman spectra. The scaling universal exponents describing the percolation transition from an insulating, 100 % transparent state, to a transparent, conducting state are consistent with the two-dimensional (2D) percolation model. These findings provide a framework for engineering the optical and electrical properties of graphene networks for technological applications where flexibility, transparency, and conductivity are required.

Introduction

Graphene is one of the most exciting materials being investigated today. It is a two-dimensional single sheet of a hexagonal lattice of carbon atoms that represents a fundamental allotrope of all graphitic forms, including fluorenes, carbon nanotubes and graphite [1]. Besides high optical transparency and conductivity [2], single and bi-layer graphenes exhibit unique electronic properties such as a room temperature fractional quantum Hall effect, ambipolar field effect and ballistic conduction [3]. A solution processed graphene material sparks wide interest as an attractive alternative for applications in conductive transparent films and scalable graphene devices [4].

For solution phase growth it is important to characterize the structure of graphene flakes in liquid suspension. Geometrical dimensions, polydispersity, spacing, and concentration are the key parameters that affect the network formation and functional properties of the resulting graphene films. A number of methods have been developed to date to obtain and process large graphene films from solution [4, 5]. The oxidation of graphite leads to intercalated graphite–oxide, which can be readily dispersed in polar solvents. These materials are not completely exfoliated and contain domains of graphitic layers [6]. Thermal exfoliation of the intercalated material yields single graphene sheets [7], which can be conveniently purified and deposited on a variety of substrates to form thin films [8]. Graphite–oxide is electrically non-conducting.

Chemical reduction recovers conductivity [7, 8], which is typically somewhat lower than that of pure graphene, due to defects and disorder [9, 10]. Significant improvement in the quality of chemically derived graphene sheets has been recently reported, where an application of organic solvents resulted in stable suspensions of single-layer graphene sheets [11, 12].

In the present work we characterize the liquid suspension of graphene sheets by multiple angle dynamic light scattering. We demonstrate the feasibility of depositing graphene films on substrates, and delineate methods to determine the collective universal properties of these films, such as the formation of percolated networks, and transparency and conductivity.

Materials and Methods[1]

In this work we used conductive foliated graphene sheets (CFGS) obtained through thermal expansion of natural graphite [6, 7]. We prepared stable dispersions of graphene sheets in chloroform by using sonication and centrifugation to purify the suspension and remove larger aggregates.

Multiple angle dynamic light scattering (MADLS) measurements were done with a Brookhaven Instruments BI-200SM laser light scattering system. A Coherent Verde 532 nm diode-pumped solid state laser was used for excitation. The laser power was set to 20 mW for all experiments. Two vertically aligned Glan-Thompson polarizers we installed in front of the laser and detectors. Round bottom borosilicate glass tubes of 12 mm diameter were used to hold 3 ml of graphene dispersion in chloroform. All measurements were done at 25 °C stabilized sample temperature. Scattering angles from 20° to 130° were chosen with a 10° interval. Twelve consecutive 5-min measurements were taken at every angle and fitted individually. The photon count of two detectors was cross-correlated in the time range from 2 μs to 10 s.

Raman spectra were collected using a micro-Raman system with an excitation laser wavelength of 1064 nm for solutions and 514.5 nm for deposits. The spot size of the laser was about 2 μm and the incident power was about 3mW.

The exfoliated materials were deposited from chloroform suspensions on the surface of alumina membranes, with 0.05 μm diameter pore size (Millipore), via a vacuum filtration process. The deposit formed a random network on the surface of the membrane. The optical characteristics of the films were determined by measuring diffuse reflectance at normal incidence in the wavelength range of 300 nm to 1200 nm, using a Perkin Elmer Lambda 950 spectrophotometer equipped with the diffuse reflectance kit [14]. The combined relative uncertainty in the reported transmittance and reflectance data are within 1 %. To measure the electrical characteristics of the network films, a comb gold electrode pattern was deposited directly on top of the network through a shadow mask. Electrical measurements were analyzed in terms of complex impedance, yielding the impedance magnitude $|Z^*|$ and the corresponding phase angle (θ) over the frequency range of 40 Hz to 10 MHz by using a four-terminal fixture attached to an Agilent 4294A precision impedance analyzer [14]. Here we report the real part of sheet conductance (σ_s) determined at 200 Hz. The lowest values of σ_s obtained for our test structure without graphene was in the range of about 10^{-10} S. All measurements were done in an inert Argon atmosphere at room temperature. The combined relative experimental uncertainty of the measured sheet conductance, σ_s, was within 4 %.

---

[1]Certain commercial equipment and materials are identified in this paper in order to specify adequately the experimental procedure. In no case does such identification imply recommendations by the National Institute of Standards and Technology nor does it imply that the material or equipment identified is necessarily the best available for this purpose.

Results and Discussion

Multiple angle dynamic light scattering performed on suspensions at a concentration of 3.3 µg/ml in chloroform shows a bimodal relaxation time distribution at all scattering angles according to CONTIN algorithm [15] so a dual exponential decay fit was successfully applied. The fast mode relaxation rate was analyzed using a model of a dilute suspension of infinitely thin rigid discs [16] utilizing diffusion coefficients of an extremely oblate ellipsoid, independent on its minor axis [17, 18]. Fig. 1 illustrates the dependence of the fast mode relaxation rate on the squared scattering vector. The linear fit has a slope of 0.46 µm²/s corresponding to the mean diameter of the platelets of 3.5 µm.
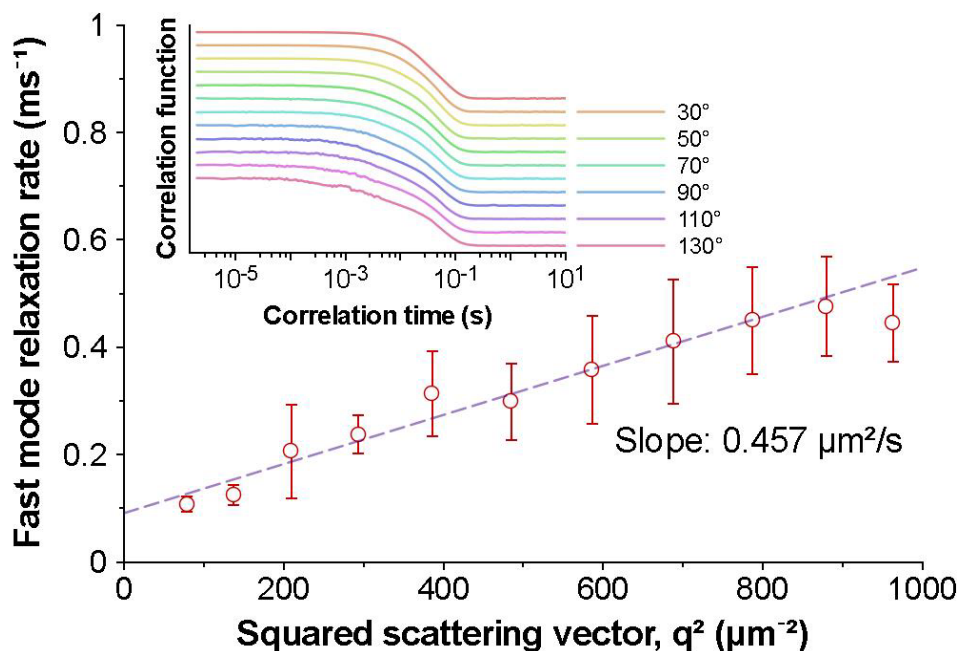
Figure 1. Fast mode relaxation rate of graphene dispersion in chloroform at a concentration of 3.3 µg/ml as measured by MADLS. Circles are the average of 12 consecutive 5-min measurements and error bars are one standard deviation. A dashed line is a linear fit according to the theory of DLS of dilute suspension of thin disks [16]. Inset shows normalized DLS correlograms of graphene dispersion in chloroform at a concentration of 3.3 µg/ml at 20 mW laser excitation and various scattering angles; curves are shifted vertically for clarity.

This agrees well with the small angle neutron scattering results fitted to a disk model, indicating that the diameter of the platelets is in the range of about 3 µm to 4 µm [19]. The slow mode relaxation rate was independent on the scattering vector and had an average value of 10.5 s^{-1}. It can be attributed to light scattered by graphene aggregates that were not completely dispersed during the sonication stage.

Representative transmission electron microscope (TEM) images (Fig. 2) show evidence of individual graphene sheets. The sheets have an irregular shape with apparent

folding and bending. Corrugations are typically 1 μm long. Elasticity theory predicts that an ideal two-dimensional membrane is unstable at finite temperatures, and therefore 2D
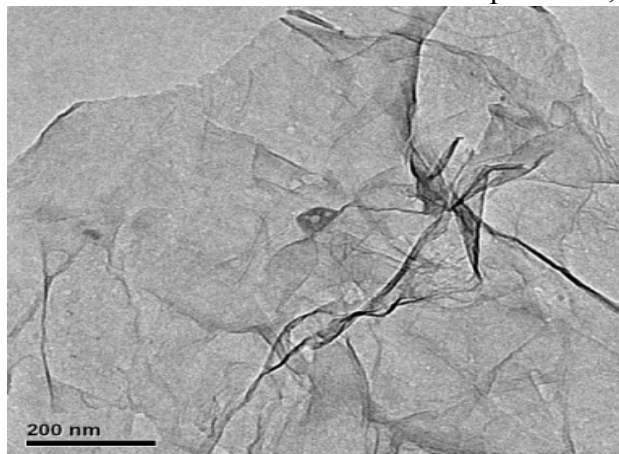
Figure 2. TEM image of graphene sheets from liquid exfoliation of graphite.

structures such as graphene develop buckling [20, 21]. Experimental reports showed that a free-hanging graphene sheet is buckled rather than flat [22]. Monte Carlo simulations suggest at the equilibrium the sheet spontaneously forms a characteristic wavelength of about 8 nm at finite temperature [23]. The amplitude of the buckling increases with the size of the membrane, because the restoring strain energy for a given deflection perpendicular to the membrane decreases with system size. Therefore, only small nano-scale membranes are predicted to stay approximately flat, whereas micrometer size membranes would have ripples and infinite membranes would break up into smaller, finite membranes as a result of the thermal vibrations [21]. The calculated amplitude of the ripples is in the range of 1 Å, which is smaller then that that seen in Fig. 2. The topographical disorder in our samples is considerable and gives rise to a relatively large amplitude of the D band on the Raman Spectrum (Fig. 3).
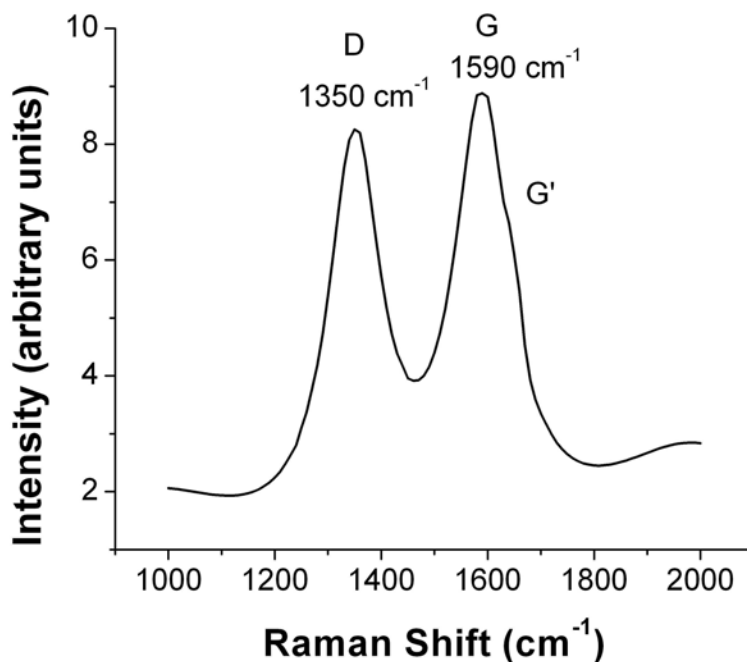
Figure 3. Raman spectra of graphene networks.

The major Raman features, common to all graphene samples, are a D band at 1350 cm^{-1}, and a G band at 1590 cm^{-1}. The D band is related to the presence of sp3 hybridized carbons and edge defects. The G band is related to the in-plane vibration of sp^2 carbon atoms. This is a doubly degenerate phonon mode at the Brillouin zone center. We also observe a 2 D band at 2683 cm^1 (not shown), which originates from a two phonon double resonance Raman process [24, 25].

Figure 4 shows the correlation plot between the sheet conductivity (σ_s) and optical transmittance (T) at a wavelength of 700 nm. It demonstrates that when the optical transparency approaches a critical value, above 80 %, the conductivity decreases dramatically.
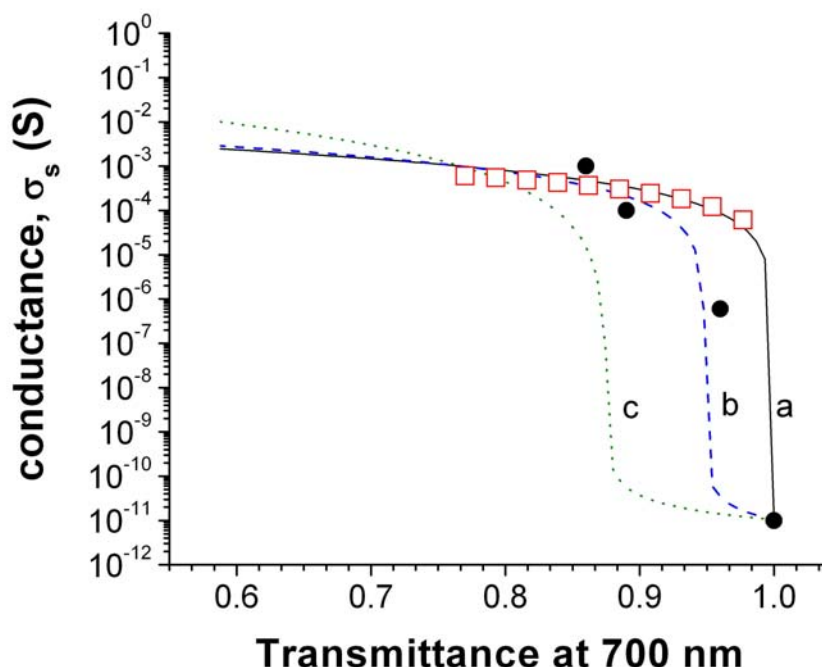
Figure 4. Sheet conductance (σ_s) and transparency (T) of graphene networks (closed circles). Lines represent calculated conductivity of percolated networks on two dimensions for the following disk diameter: (a) solid line 3 μm; (b) dashed line 1.5 μm and (c) dotted line 0.5 μm. The open squares represent calculated optical properties of graphene (T=0.977) and multilayer graphene sheets.

The sheet conductance (σ_s) of our networks changes by seven orders of magnitude, from 5×10^{-3} S to about 5×10^{-7} S, while the transparency increases from 85 % to about 95 %. Results shown in Fig. 4 indicate that the interconnectivity distance is between 2 μm and 3 μm. Our σ_s values in the saturation regime, where the transmittance is below 80 %, are in the range of about 0.005 S, which is comparable to the conductivity predicted for a 10 graphene layer thick film. Our results are also comparable to that reported for transparent electrode materials made of carbon nanotubes [14, 26]. The overall character of the conductivity plots at transparency above 90 % is characteristic of a percolation transition. With increasing interconnectivity length, the network conductivity increases and the percolation conditions for σ_s shift to higher *T*, while the crossover transition from the insulating to the conducting state occurs in a narrower transmittance range. We determined the critical percolation exponents (*s* and *t*) in relation to the interconnectivity length by analyzing the σ_s and *T* data in terms of the generalized effective medium theory (GEM) [27]. The conductivity of the network in the high concentration limit is equivalent to that of multilayer graphene sheets [28]. The value of σ_s depends on the contact resistance and other factors that are not addressed in the simple GEM model. The critical percolation exponents parameters are close to those theoretically expected for a large conducting 2D network, [29] where *s* = *t* =1.3. Thus, we find experimental evidence that our graphene networks can be described as nearly two-dimensional and that GEM percolation theory provides a quantitative description of conductivity changes in these materials through the conductivity–transparency

percolation transition. These observations indicate that considerable insight and control of the conductivity and optical properties can be obtained by adjusting the size, concentration, and polydispersity of the graphene platelets. The GEM percolation theory provides a convenient framework for describing and engineering these changes for nanotechnology applications, exploiting these novel materials.

References

1. C. N. R. Rao, K. Biswas, K. S. Subrahmanyam, and A. Govindaray. J. Mater. Chem. **19**, 2457 (2009).

2. A. B. Kuzmenko, E. van Heumen, F. Carbone and D. van Marel, *Phys. Rev. Lett.*, **100**, 117401 (2008).

3. R. R. Nair, B. Blake, A. N. Grigeronko, K. S. Novoselov, T. J. Booth, T. Stauber, N. M. R. Peres, A. K. Geim, *Science*, **320**, 1308 (2008).

4. S. Stankowich, D. A. Dikin, G. H.B. Dommet, K. M. Kohlhaas, E. J. Zimney, E A. Stach, R. D. Piner, S. T. Nguyen and R. S. Ruoff, *Nature Lett.*, **442**, 282 (2006).

5. D. Li, M. B. Muller, S. Gilje, R. B. Kaner, and G. G. Wallace, *Nature Nanotech.***3**, 101 (2008).

6. H. C. Schniepp; J. L.Li, M. J. McAllister, J. Sai, M. Herrera-Alonso, D. H. Adamson, R. K. Prud'homme, R. Car, D. A. Saville, I. A. Aksay, *J. Phys. Chem. B* **110**, 8535 (2006).

7. M. J. McAllister, J. L. Li,| D. H. Adamson, H. C. Schniepp, A. A. Abdala, J. Liu, M. Herrera-Alonso, D. L. Milius, R. Car, R. K. Prud'homme, and I. A. Aksay, *Chem. Mater*. **19,** 4396 (2007).

8. G. Eda, G. Fanchini, M. Chhowalla, *Nature Nanotech Adv. Pub.*, 1 (2008).

9. X. Li, G. Zhang, X. bai, X. Sun, X. Wang, E. Wang, and H. Dai, *Nature Nanotech. Lett.*, **3** 538 (2008).

10. H. A. Becerril, J. Mao, Z. Liu, R. M. Stoltenberg, Z. Bao, Y. Chen, *ACS Nano*, **3**, 463 (2008).

11. Y. Hernandez, V. Nicolosi, M. Lotya, F. M. Blighe, Z. Sun, S. De, I. T. McGovern, B. Holland, M. Byrne, Y. K. Gun'ko, J. J. Boland, P. Niraj, G. Deusberg, S. Krishnamurthy, R. Goodhue, J. Hutchison, V. Scardaci, A. Ferrari and J. N. Coleman, *Nature Nanotech,* **3**, 563 (2008).

12. C. Valle's, C. Drummond,† H. Saadaoui, C. A. Furtado, M. He,O. Roubeau,†L. Ortolani, M. Monthioux, and A. Pe´nicaud, *J. Am. Chem. Soc*. **130**, 15802 (2008).

13 J. Lu, J. Yang, J. Wang, A. Lim, S. Wang, and K. P. Loh, *ACS NANO* **3**, 2367 (2009).

14. D. Simien, J. A. Fagan, W. Luo, J. F. Douglas, K. Migler and J. Obrzut, *ACS NANO*, **2**, 1879 (2008).

15. S. W. Provencher, Computer Physics Comm. **27**, 229 (1982).

16. S. Fujime and K. Kubota, Biophys. Chem. **23**, 1 (1985).

17. B. J. Frisken, Appl. Optics **40**, 4087 (2001).

18. K. Kubota, Y. Tominaga, S. Fujime, J. Otomo, and A. Ikegami, Biophys. Chem. 23, 159 (1985).

19. M. Yoonessi, R. Vilkin, J. Gaier, to be published.

20. D. R. Nelson, and L. Peliti, *J. Phys*. **48,** 1085 (1987).

21. Doussal, P. & Radzihovsky, L. *Phys. Rev. Lett.* **69,** 1209–1212 (1992).

22. J. C. Meyer, *et al. Nature* **446,** 60–63 (2007).

23. A. Fasolino, J. H. Los, and M. I. Katsnelson, *Nature Mat.* **6,** 858 (2007).

24. A. K. Gupta, T. J. Russin, H. R. Gutierrez, P. C. Eklund, , *ACS NANO* **3**, 45 (2009).

25. Z. H. Ni; T. Yu, Z. Q. Luo, Y. Y. Wang, L. Liu, C. P. Wong, J. Miao, W. Huang, Z. X. Shen, , *ACS NANO* **3**, 569 (2009).

26 J. L. Blackburn, T. M. Barnes, M. C. Beard, Y. H. Kim, R. C. Tenent, J. McDonald, B. To, T. J. Coutts, M. J. Heben, *ACS NANO* **2**, 1266 (2008).

27.D. S. McLachlan, W. D. Heiss, C. Chiteme, J. Wu, *Phys. Rev.* **B 58**, 13558 (1998).

28. J. Obrzut and K. B. Migler, *ECS Trans*. **19**, 69 (2009).

29. P. Lajko, L. Turban, *J. Phys. A: Math. Gen.* **33**, 1683 (2000).